

Magnetic vortices in layered superconducting slabs

A. Yu. Martynovich

Donetsk Physical-Technical Institute, 340114 Donetsk, Ukraine

(Submitted 30 March 1993)

Zh. Eksp. Teor. Fiz. **105**, 912–927 (April 1994)

It is shown that a tilted magnetic field penetrates into a superconducting slab in the form of bent vortices. The equilibrium shapes of the vortices and of the vortex lattice depend on the orientation of the external field, the degree of anisotropy of the crystal, and the slab thickness. In very thin films, rectilinear tilted vortices form a hexagonal lattice oriented symmetrically with respect to the external field. Near the surface of a thick slab each vortex is directed along the normal to the surface, and inside the slab it is tilted toward the planar component of the field. Long-range repulsion and short-range attraction of the bent vortices in a thick slab give rise to unusual vortex structures. The transformation of these structures in superconductors with different degrees of anisotropy is described for a tilted external field, and the existence of metastable vortex lattices in strongly anisotropic crystals is demonstrated. Within the framework of the proposed theory an explanation is given of the results of experiments which visualize the vortex structures in $\text{YBa}_2\text{Cu}_3\text{O}_x$ and $\text{Bi}_2\text{Sr}_2\text{CaCu}_2\text{O}_x$ slabs.

1. INTRODUCTION

A few years ago a series of papers appeared reporting measurements of the torque of layered superconductors in a strong magnetic field.^{1–3} These papers demonstrated beautiful agreement between theory¹ and experiment^{2,3} and confirmed the possibility of using the anisotropic Ginzburg–Landau theory⁴ to describe the new high-temperature superconductors (HTSC). The use of this theory proved to be especially fruitful in the description of magnetization processes in HTSC crystals. Thus, for the case in which the external field is aligned with one of the anisotropy axes both isolated vortex⁵ and vortex lattice^{6,7} structures were predicted, and experiments confirmed both the first⁸ and the second of these results.^{9,10} The magnetic structure of a HTSC varies substantially with the tilt of the external field from the symmetry axis. The most striking peculiarity of tilted vortices in unbounded HTSC crystals is inversion of the longitudinal vortex field,^{10,11} which results in mutual attraction between the vortices and their formation into chains.^{10,12} For small values of the magnetic induction B the vortex spacing in the chains is almost constant and much less than the interchain distance, which varies inversely with B . The intervortex attraction lowers the eigen-energy of the chain in such a way that two types of chains can coexist in strongly anisotropic HTSC's.¹⁰ For a fixed orientation of the external field these chains differ in the tilts of the vortices and the periods of the chains.

Vortex chains were discovered experimentally on the surface of single crystals of $\text{YBa}_2\text{Cu}_3\text{O}_x$ [YBCO(123)] (Ref. 13) and $\text{Bi}_2\text{Sr}_2\text{CaCu}_2\text{O}_x$ [BSCCO(2212)] (Ref. 14) with the help of the decoration technique in which fine ferromagnetic particles are dispersed over the surface of the sample to reveal the magnetic flux pattern at the surface. However, in the given case there is a substantial dif-

ference between theory and experiment. Thus, in Ref. 10 it was shown that dense chains can be observed when the angle of the external field θ tilts less than 5° . But in reality the chains are observed only at significantly larger tilt angles. Moreover, in the indicated tilt angle interval only a hexagonal vortex lattice is observed, whose existence completely contradicts theory.¹⁵ The theory predicts the coexistence of vortex chains when the external field tilt angle is less than 10^{-2} degrees. In the experiments both chains and a hexagonal lattice were observed simultaneously¹⁴ at $\theta \sim 60^\circ$. At smaller tilt angles only a weakly deformed hexagonal structure was visualized.

In our view, this disagreement is due to a difference in the objects of study. The experiments are always carried out on laminar samples, but the theory considers unbounded superconductors. An elementary analysis immediately reveals a fundamental difference in the results obtained when the finite thickness of the sample is taken into account. The interaction of the vortices in vacuum should lead to a long-range repulsion, falling off with intervortex distance R as $1/R$ (Ref. 16). This repulsion should order the vortices into a sparse hexagonal lattice which can deform with increasing magnetic induction, thanks to the anisotropic short-range interaction of the tilted vortices. The present paper is dedicated to a detailed study of the effect of finite thickness of the HTSC crystal on its magnetic properties. Section 2 contains a statement of the problem and a general expression for the field of an isolated vortex of arbitrary shape. In Section 3 the Gibbs potential is obtained for a superconducting slab in a tilted magnetic field. The structure of the vortex field in a thin film is described in Section 4. Section 5 contains a description of the equilibrium shape of a vortex thread and the vortex interaction in a thick slab. Section 6 presents results of a numerical calculation of the vortex structures in

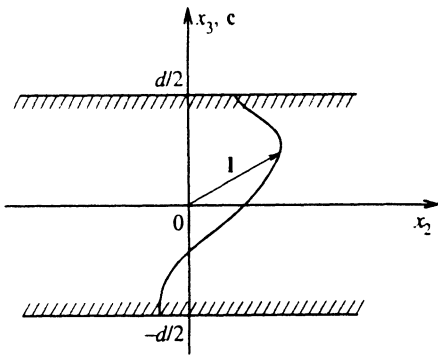


FIG. 1. Sketch of the investigated slab geometry. The slab occupies the region $|x_3| < d/2$, the surface layers are hatched. The vortex line is given by the vector function $\mathbf{l}(x_3)$.

YBCO(123) and BSCCO(2212) slabs. In the Conclusion we discuss the most striking features of the elastic properties of vortex structures in HTSC slabs.

2. MAGNETIC STRUCTURE OF A BENT VORTEX

Let us consider the following problem geometry (see Fig. 1). A superconducting slab of thickness d is centered in the x_1x_2 plane. The slab has two external surfaces $x_3 = \pm d/2$ and is unbounded in the x_1 and x_2 directions. The anisotropy axis \mathbf{c} is aligned with the normal \mathbf{n} to one of the surfaces of the slab. An isolated vortex thread cuts through the slab from one surface to the other, and the center of the vortex coincides with some arbitrary line $\mathbf{x} = \mathbf{l}(x_3)$.

To determine the magnetic field $\mathbf{h}(\mathbf{x})$ created by the vortex over all space, we solved the system of Maxwell equations

$$\text{div } \mathbf{h} = 0, \quad \text{rot } \mathbf{h} = 0 \quad (1)$$

outside the superconductor and London equations

$$\mathbf{h} + \lambda^2 \text{rot } \hat{\mu} \text{rot } \mathbf{h} = \phi_0 \int d\mathbf{l} \delta(\mathbf{x} - \mathbf{l}(x_3)) \quad (2)$$

inside. Here λ is the penetration depth of the magnetic field in the superconductor, ϕ_0 is the flux quantum, and $\hat{\mu}$ is the dimensionless effective mass tensor. In a single-axis superconductor the principal values of $\hat{\mu}$ are $\mu_a = \mu_b$ and $\mu_c = \mu_a^{-2}$.

The standard Fourier transform method assuming continuity of the field at the interfaces leads to the following vortex field distribution:

$$\mathbf{h}(\mathbf{x}) = \frac{\phi_0}{8\pi^2} \int d^2\mathbf{q} \mathbf{h}^F(\mathbf{q}, x_3) \exp(i\mathbf{q}\mathbf{x}). \quad (3)$$

Here and below we take $\lambda_a = \lambda \mu_a^{1/2}$ as the unit length and we normalize the wave vector \mathbf{q} by λ_a^{-1} , where $\mathbf{q} = (q_1, q_2, 0)$ is a two-dimensional vector in the plane of the slab.

Outside the superconductor we have

$$\mathbf{h}^F(\mathbf{q}, x_3) = \eta \int_{-d/2}^{d/2} dl_3 \left[\frac{\text{ch}(Q_2 l_3)}{f_2(q)} \pm \frac{\text{sh}(Q_2 l_3)}{f_1(q)} \right] \times \exp \left[-i\mathbf{q}\mathbf{l} + q \left(\frac{d}{2} - |x_3| \right) \right].$$

Here $\eta = (\mp iq_1/q, \mp iq_2/q, 1)$, and the upper and lower signs correspond to the field distribution above the slab and below it. In expression (4) we have made use of the following notation:

$$q = (q_1 + q_2)^{1/2}, \quad Q_2 = (1 + q^2)^{1/2},$$

$$f_1(q) = q \text{sh} \left(Q_2 \frac{d}{2} \right) + Q_2 \text{ch} \left(Q_2 \frac{d}{2} \right),$$

$$f_2(q) = q \text{ch} \left(Q_2 \frac{d}{2} \right) + Q_2 \text{sh} \left(Q_2 \frac{d}{2} \right).$$

Outside the superconductor the field $\mathbf{h}^F(\mathbf{q}, x_3)$ has the following components:

$$h_3^F(\mathbf{q}, x_3) = \frac{1}{Q_2} \int dl_3 \left[-\text{sh}(Q_2 |x_3 - l_3|) + \frac{f_1(q)}{f_2(q)} \text{ch}(Q_2 l_3) \text{ch}(Q_2 x_3) - \frac{f_2(q)}{f_1(q)} \text{sh}(Q_2 l_3) \text{sh}(Q_2 x_3) \right] \exp(-i\mathbf{q}\mathbf{l});$$

$$h_1^F(\mathbf{q}, x_3) = q_1 A_1 + q_2 A_2,$$

$$h_2^F(\mathbf{q}, x_3) = q_2 A_1 - q_1 A_2,$$

$$A_1(\mathbf{q}, x_3) = \frac{1}{q^2} \int (d\mathbf{l} \cdot \mathbf{q}) J(x_3, l_3, Q_2) \exp(-i\mathbf{q}\mathbf{l})$$

$$- \frac{i}{q} \int dl_3 \left[\frac{\text{sh}(Q_2 l_3) \text{ch}(Q_2 x_3)}{f_1(q) \text{ch}(Q_2 d/2)} \right.$$

$$\left. + \frac{\text{ch}(Q_2 l_3) \text{sh}(Q_2 x_3)}{f_2(q) \text{sh}(Q_2 d/2)} \right] \exp(-i\mathbf{q}\mathbf{l}),$$

$$A_2(\mathbf{q}, x_3) = \frac{1}{q^2} \int (q_2 dl_1 - q_1 dl_2) J(x_3, l_3, Q_1) \exp(-i\mathbf{q}\mathbf{l}),$$

$$J(x, l, Q) = \frac{1}{Q} \left[\exp(-Q|x-l|) + \frac{\exp(-Qd) \text{ch}(Q|x-l|) - \text{ch}(Q|x+l|)}{\text{sh}(Qd)} \right],$$

$$Q_1 = (1 + \mu_a^{-3} q^2)^{1/2}.$$

The magnetic field distribution (3) satisfies the following conditions. For arbitrary curvature of the vortex the magnetic flux $\phi = \int \mathbf{nh} dx_1 dx_2$ through any plane of constant x_3 is equal to ϕ_0 . Analogous integrals of the planar components of the field are always equal to zero outside the slab, and inside it (for $|x_3| < d/2$) the values of the integrals depend on the shape of the vortex thread. In general the vortex field is characterized by two decay parameters, λ_a

and $\lambda_c = \lambda_a \mu_a^{-3/2}$. For a rectilinear vortex with $l \parallel n$ we have $A_2(\mathbf{q}, x_3) = 0$ and the magnetic field depends only on λ_a . The normal component of the vortex current

$$j_3(\mathbf{x}) = -\frac{ic\phi_0}{8\pi} \int \frac{d^2q}{4\pi^2} q^2 A_2(\mathbf{q}, x_3) \quad (4)$$

depends only on λ_c and always vanishes at the outer boundaries of the slab. Only in the case of a rectilinear vortex perpendicular to the surface does $j_3(x) = 0$ hold.

3. THE GIBBS POTENTIAL OF A SUPERCONDUCTING SLAB

Let us consider a HTSC slab in an external uniform magnetic field

$$\mathbf{H} = n\mathbf{B} + \mathbf{H}_2,$$

where the planar component of the field \mathbf{H}_2 is aligned with the x_2 axis. The influence of the tilted field \mathbf{H} on the vortex state of a film reduces to two effects. The normal component $n\mathbf{B}$ penetrates into the superconductor in the form of Abrikosov vortices with mean vortex concentration $\langle n_L \rangle = B/\phi_0$. The tangent component \mathbf{H}_2 penetrates into the superconductor in the form of the Meissner field

$$\mathbf{h}_M = \mathbf{H}_2 \frac{\text{ch}(x_3)}{\text{ch}(d/2)} \quad (5)$$

but only to distances of order λ_a . Acted upon by the field \mathbf{H}_2 the vortices in the slab become bent, and their equilibrium shape $l(x_3)$ is determined from the minimum of the Gibbs potential

$$G = F - \int \frac{d^3x}{4\pi} \mathbf{H}_2 \mathbf{h}. \quad (6)$$

In the London limit the free energy of the slab

$$F = \int \frac{d^3x}{4\pi} [h^2 + \mu_a^{-1} \text{rot } \mathbf{h} \cdot \hat{\mu} \cdot \text{rot } \mathbf{h}] \quad (7)$$

is expressed in terms of a superposition of the vortex fields and the Meissner field:

$$\mathbf{h} = \sum_i \mathbf{h}(\mathbf{x} - l^i) + \mathbf{h}_M(x_3).$$

We neglect the energy of the Meissner field and currents as a small constant. Using the integral representations of the components of the vortex field (3) we write the free energy in the form

$$F = \left(\frac{\phi_0}{4\pi}\right)^2 \sum_i \sum_j \int \frac{d^2q}{4\pi} \iint \mathcal{D}(l^i, l^j) \exp[iq(l^j - l^i)], \quad (8)$$

which contains a double sum over all the vortices with indices i and j ; \mathcal{D} is the Fourier transform of the interaction energy of the two vortex segments dl^i and dl^j :

$$\begin{aligned} \mathcal{D}(l^i, l^j) = & dl_3^i dl_3^j \left[\frac{\text{ch}(Q_2 l_3^i) \text{ch}(q l_3^j)}{f_2(q) \text{sh}(q d/2)} + \frac{\text{sh}(Q_2 l_3^i) \text{sh}(q l_3^j)}{f_1(q) \text{ch}(q d/2)} \right] \\ & + dl_3^i dl_3^j \frac{1}{Q_2} \left[-\text{sh}(Q_2 |l_3^i - l_3^j|) + \frac{f_1(q)}{f_2(q)} \right] \end{aligned}$$

$$\begin{aligned} & \times \left[\text{ch}(Q_2 l_3^i) \text{ch}(Q_2 l_3^j) - \frac{f_2(q)}{f_1(q)} \text{sh}(Q_2 l_3^i) \text{sh}(Q_2 l_3^j) \right] \\ & + (\mathbf{q} \cdot dl^i)(\mathbf{q} \cdot dl^j) \frac{1}{q^2} J(l_3^i, l_3^j, Q_2) \\ & + (q_2 dl_1^i - q_1 dl_2^i)(q_2 dl_1^j - q_1 dl_2^j) \frac{1}{q^2} J(l_3^i, l_3^j, Q_1) \\ & + idl_3^i (\mathbf{q} \cdot dl^j) \frac{1}{q} \left[\frac{\text{ch}(Q_2 l_3^j)}{f_2(q)} \left[\frac{\text{sh}(q l_3^j)}{\text{sh}(q d/2)} \right. \right. \\ & \left. \left. - \frac{\text{sh}(Q_2 l_3^j)}{\text{sh}(Q_2 d/2)} \right] + \frac{\text{sh}(Q_2 l_3^j)}{f_1(q)} \left[\frac{\text{ch}(q l_3^j)}{\text{ch}(q d/2)} \right. \right. \\ & \left. \left. - \frac{\text{ch}(Q_2 l_3^j)}{\text{ch}(Q_2 d/2)} \right] \right]. \quad (9) \end{aligned}$$

In expression (9) we have used the same notation as in the definition of the vortex field (3). The results (8) and (9) are quite general. In the limit of an isotropic unbounded superconductor, they go over to well-known expressions.¹⁷ We will consider the particular cases of a thin film ($d \ll \lambda_a$), a thick slab ($d \gg \lambda_a$), and an HTSC which is unbounded below. Note that as in the case of rectilinear vortices parallel to the surface,¹⁸ the free energy (8) does not contain any terms describing the interaction of the vortices with the Meissner field.

The last integral term in the Gibbs potential (6) has the form

$$- \int \frac{d^3x}{4\pi} \mathbf{H}_2 \mathbf{h} = -\frac{\phi_0 H_2}{4\pi} \sum_i \int dl_2^i \left[1 - \frac{\text{ch}(l_3^i)}{\text{ch}(d/2)} \right]. \quad (10)$$

It is well known¹⁸ that the magnetic flux ϕ_v of a rectilinear vortex, parallel to the plane of the slab, differs from the flux quantum ϕ_0 and is equal to

$$\phi_v = \phi_0 \left[1 - \frac{\text{ch}(l_3^i)}{\text{ch}(d/2)} \right]. \quad (11)$$

Consequently, expression (9) can be treated as the energy of interaction with the field \mathbf{H}_2 of the bent vortices, each element dl_2^i (but not dl^i) of which has the coordinate l_3^i and transfers flux ϕ_v given by (11).

4. VORTICES IN A THIN FILM

1. In thin superconducting films ($d \ll \lambda_a$) one can assume that the magnetic vortices are rectilinear and tilted with respect to the normal \mathbf{n} by some angle. It is convenient to describe tilted vortices by the vector κ whose direction coincides with the projection of the vortex axis on the plane of the film, and whose magnitude is equal to the tangent of the tilt angle. The components of the vector $l(x_3)$, which describes the shape of the vortex line, are equal to

$$l_3 = x_3, \quad l_i = R_i + \kappa_i x_3, \quad i = 1, 2.$$

The free energy of the thin film has the form

$$F = \left(\frac{\phi_0}{4\pi}\right)^2 \sum_i \sum_j \exp[i\mathbf{q}(\mathbf{R}^j - \mathbf{R}^i)] \int \frac{d^2q}{4\pi} \iint \mathcal{D}(l^i, l^j) \times \exp[i\mathbf{q}(\kappa^j l_3^j - \kappa^i l_3^i)], \quad (12)$$

$$\mathcal{D}(l^i, l^j) = dl_3^i dl_3^j \left[\frac{2}{qd(q+d/2)} + (\kappa^i \mathbf{q})(\kappa^j \mathbf{q}) \frac{1}{q^2} \times J(l_3^i, l_3^j, Q_2) + [\kappa^i \mathbf{q}][\kappa^j \mathbf{q}] \frac{1}{q^2} J(l_3^i, l_3^j, Q_1) \right].$$

Here we have assumed that the tilts of the vortices can be different.

In the double sum in (12) the terms with $i=j$ describe the eigen-energy of the vortices

$$F_0 = d \left(\frac{\phi_0}{4\pi}\right)^2 \left[\ln\left(\frac{2}{d\xi}\right) + \frac{\kappa^2}{2} (1 + \mu_a^{3/2}) \ln\left(\frac{d}{\xi}\right) \right]. \quad (13)$$

The energy of the pairwise vortex interaction [$i \neq j$ in (12)] depends on the vector $\mathbf{R} = \mathbf{R}^i - \mathbf{R}^j$ connecting the vortices in the plane of the film. In the case in which the vortex tilts are equal the interaction potential is equal to

$$U(\mathbf{R}) = d \left(\frac{\phi_0}{4\pi}\right)^2 \left\{ \frac{\pi}{2} \left[H_0\left(\frac{Rd}{2}\right) - Y_0\left(\frac{Rd}{2}\right) \right] + \frac{d^2}{6R^3} [3(\kappa_1^2 R_1^2 + \kappa_2^2 R_2^2) - \kappa^2 R^2] + \left[\frac{(\kappa \mathbf{R})^2}{R^2} + \frac{\kappa^2 d}{2\sqrt{3}R} \right] K_0\left(\sqrt{3} \frac{2R}{d}\right) + \mu_a^3 \left[\frac{[\kappa \mathbf{R}]^2}{R^2} - \frac{\mu_a^{3/2} \kappa^2 d}{2\sqrt{3}R} \right] K_0\left(\sqrt{3\mu_a^3} \frac{2R}{d}\right) \right\}. \quad (14)$$

Here the first term inside the braces, proportional to the difference of the Struve function $H_0(x)$ and the Neumann function $Y_0(x)$, dominates. In contrast to the remaining terms, it describes the long-range action of the vortices in the film¹⁶ and does not depend on the parameters κ and μ_a . The last two terms, containing the modified Bessel function $K_0(x)$, are substantially short-range. Their contribution becomes noticeable only for $R < d$, i.e., in large external fields whose magnitude satisfies $B > \phi_0 d^{-2}$. For $d = 0.1 \mu\text{m}$ the limiting value of the magnetic induction is 2000 G. In smaller fields these last two terms can be neglected; then all dependence on μ_a disappears from expression (14). Thus, over a wide interval of fields, the vortex-vortex interaction in the film does not depend on the anisotropy parameters.

2. Here we will describe the equilibrium vortex lattice. The vortex-vortex interaction in a film, to within small terms of order $\kappa^2 d^3 R^{-2}$, is centrally symmetric. This fact underlies the existence of a hexagonal equilibrium vortex lattice. The stability of such a structure in the case $\kappa = 0$ was demonstrated earlier.¹⁹ In this case a degeneracy of the free energy F with respect to the orientation of the unit cell in the plane of the film is observed. In a tilted magnetic field this degeneracy is removed and the lattice orients itself symmetrically with respect to the field \mathbf{H}_2 . In a stable lattice one of the elementary translation vectors is perpendicular to the field \mathbf{H}_2 and the vector κ .

The equilibrium tilt of the vortices is determined by the condition for the minimum of the Gibbs potential

$$G = F - \frac{\phi_0 H_2 d}{4\pi} \left[1 - \left(\frac{2}{d}\right) \text{th}\left(\frac{d}{2}\right) \right] \sum_i \kappa_i. \quad (15)$$

In the free energy F both the vortex eigen-energy (13) and the interaction potential (14) depend on κ . Minimizing E with respect to κ_1 and κ_2 , we obtain

$$\kappa_1 = 0, \quad (16)$$

$$\kappa_2 = \frac{H_2}{3} \left[\frac{1 + \mu_a^{3/2}}{2} H_{c1}(d) + \frac{B^{3/2}}{\pi \phi_0^{1/2}} \right]^{-1}.$$

Here $H_{c1}(d) = 2\phi_0/\pi d^2 \ln(d/\xi) \sim 1000$ G is the first critical penetration field of the rectilinear vortices in an isotropic film.¹⁸ Anisotropy decreases this value by a factor of $(1 + \mu_a^{3/2})/2 \sim 0.5$.

From the solution (16) it follows that the vortices always lie in the plane formed by the vectors \mathbf{n} and \mathbf{H} . In the case of small magnetic induction $B < \phi_0 d^{-4/3} \sim 1$ G, the term containing B and taking account of the vortex-vortex interaction can be neglected. In this case expression (16) describes the tilt of an isolated vortex. The vortex-vortex interaction always decreases this tilt.

3. Note that the tilt of the vortices is small even for $H_2 = 1 + \mu_a^{3/2}/2H_{c1}(d)$. At larger values of H_2 a film with rectilinear vortices parallel to its central plane satisfies the conditions of thermodynamic equilibrium.¹⁸ The Bean-Livingston barrier hinders the penetration of such vortices. However, the vortices that do penetrate into the film can lower their own energy by bending into a zigzag shape or as a result of unbounded lengthening of that portion of the vortex that lies in the central plane of the film. Thus, our assumption that the vortices are rectilinear in a thin film is valid only under the condition

$$H_2 < H_{c1}(d) + \frac{B^{3/2}}{\phi_0^{1/2}}. \quad (17)$$

5. VORTICES IN A THICK SLAB

1. The interaction energy of two vortex segments (9) in the case $d \gg l$ has the form

$$\mathcal{D}(l^i, l^j) = dl_3^i dl_3^j \frac{1}{Q_2} \exp(-Q_2 |l_3^i - l_3^j|) + dl_3^i dl_3^j \frac{\exp[-(d/2 - |l_3^i|)Q_2]}{q + Q_2} \times \left[\frac{\text{ch}(ql_3^i)}{\text{ch}(qd/2)} + \text{sign}(l_3^i) \frac{\text{ch}(ql_3^i)}{\text{ch}(qd/2)} \right] + (dl^i \mathbf{q})(dl^j \mathbf{q}) \frac{1}{q^2 Q_2} [\exp(-Q_2 |l_3^i - l_3^j|) - \exp[-Q_2(d - |l_3^i + l_3^j|)]] + (q_2 dl_1^i - q_1 dl_2^i)$$

$$\begin{aligned} & \times (q_2 dl_1^i - q_1 dl_2^i) \frac{1}{q^2 Q_1} [\exp(-Q_1 |l_3^i - l_3^j|) \\ & - \exp[-Q_1 (d - |l_3^i + l_3^j|)]]]. \end{aligned} \quad (18)$$

The limiting case of an unbounded superconductor¹⁷ follows from expression (18) by dropping those terms that contain the parameter d .

The interaction of vortex segments depends substantially on their arrangement within the slab. If one of these segments is located on the surface of the superconductor, $|l_3^i| = d/2$, then the terms in expression (18) proportional to dl_1 and dl_2 vanish. The remaining terms describe the exponentially weak interaction with the segment dl_3^j lying within the superconductor, and the long-range action if $l_3^j = l_3^i = \pm d/2$. An analogous result was obtained in Ref. 20 for rectilinear vortices. In the interior of the slab ($|l_3^i|, |l_3^j| < d/2 - 1$) the vortex segments interact with each other in the same way as in an unbounded superconductor.

2. We will describe the shape of a vortex by the functions

$$\kappa_1(l_3) = \frac{dl_1}{dl_3}, \quad \kappa_2(l_3) = \frac{dl_2}{dl_3},$$

analogous to the vector κ introduced in Section 4.

The eigen-energy of an arbitrary bent vortex has the form

$$\begin{aligned} F_0 = & \left(\frac{\phi_0}{4\pi}\right)^2 \int_{-d/2}^{d/2} dl_3 \left[\frac{(1 + \mu_a^3 \kappa^2) \ln(\xi^{-1})}{(1 + \mu_a^3 \kappa_1^2)^{1/2} (1 + \mu_a^3 \kappa_2^2)^{1/2}} \right. \\ & \left. + \frac{\kappa^2}{2} \exp\left(\left|l_3\right| - \frac{d}{2}\right) + (1 - \mu_a^3) \frac{\kappa^2}{2} E_1\left(\frac{d}{2} + \xi - \left|l_3\right|\right) \right]. \end{aligned} \quad (19)$$

Here $E_1(x)$ is the exponential integral function and $\kappa^2 = \kappa_1^2 + \kappa_2^2$. The first term inside the braces describes the eigen-energy of the vortex segment far from the surface of the slab and coincides with the vortex energy in an unbounded HTSC.⁴ The remaining terms are important only near the surface, $d/2 - |l_3| \leq 1$, where the influence of crystalline anisotropy on the eigen-energy of the vortex segment vanishes.

The equilibrium shape of the vortices $\kappa(l_3)$ is determined by the condition for the vanishing of the variational derivative

$$\frac{\delta G_0}{\delta \kappa_i(l_3)} = 0,$$

where

$$G_0 = F_0 - \frac{H_2}{4\pi} \int dl_3 \kappa_2(l_3) \phi_v(l_3). \quad (20)$$

The obvious solution is $\kappa_1(l_3) = 0$, and for $\kappa_2(l_3)$ we obtain the equilibrium equation

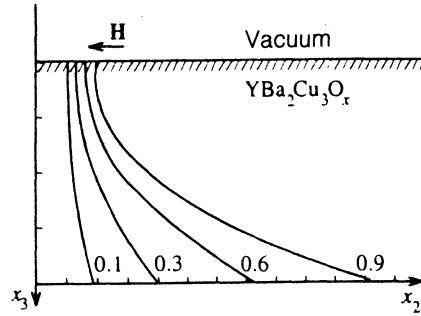


FIG. 2. Equilibrium shape of an isolated vortex near the surface of a single crystal of YBCO(123) for different values of the planar field; $\mu_a = 0.343$. The value of H_2 in units of H_{c1} is given to the right of each vortex line. The positions of the vortices at the outer surface were chosen arbitrarily. The distance between the ticks on the axes is equal to λ_a .

$$\begin{aligned} & \frac{\mu_a^3 \kappa_2^2 \ln(\xi^{-1})}{(1 + \mu_a^3 \kappa_2^2)^{1/2} + \kappa_2} \left[\exp\left(\left|l_3\right| - \frac{d}{2}\right) \right. \\ & \left. + (1 - \mu_a^3) E_1\left(\frac{d}{2} + \xi - \left|l_3\right|\right) \right] = H_2 \frac{4\pi}{\phi_0} \left[1 - \frac{\text{ch}(l_3)}{\text{ch}(d/2)} \right]. \end{aligned} \quad (21)$$

The solution $\kappa_2(l_3)$ of this equation possesses the following properties. On the surface of the superconductor we have $\kappa_2 = 0$, i.e., $\kappa_2(\pm d/2) = 0$, i.e., the ends of the vortex thread are directed precisely along the surface normal of the crystal. The vortices in superfluid helium also have such an orientation²¹ as do screw dislocations near the surface of a solid body.²² Note that edge dislocations, which do not possess radial symmetry, are directed at an angle to the surface of the crystal. Therefore we make the assumption that for an arbitrary orientation of the symmetry axis c relative to the normal \mathbf{n} the vortices near the surface of the crystal are tilted relative to \mathbf{n} .

In the center of the slab we have

$$\kappa_2(0) = \mu_a^{-3/2} [(H_{c1}/H_2)^2 - 1]^{-1/2}, \quad (22)$$

where $H_{c1} = \phi_0/4\pi\mu_a^{3/2} \ln(\xi^{-1})$ is the first critical field of rectilinear vortex generation in the central plane of the slab.

Far from the surface of the slab the tilt of the vortex line is almost constant and is given by expression (22). The transition from solution (22) to $\kappa_2(\pm d/2) = 0$ takes place at $|l_3| \approx d/2 - 1$. The shape of the bent vortex is obtained by numerical integration of the solution of Eq. (21) and is shown in Fig. 2.

From expression (22) and Fig. 2 it is clear that for $H_2 < H_{c1}$ the vortex tilt $\kappa_2(l_3)$ is finite. In the field H_{c1} we have $\kappa_2(0) = \infty$ and the vortex line loses its stability with respect to its extent along the x_2 axis. In larger planar fields the energy of the central segment of the vortex line becomes negative. The vortex lengthens without bound because the upper and lower ends move in different directions. This process can be limited only by a finite concentration of vortices, when repulsion between approaching vortices sets in.

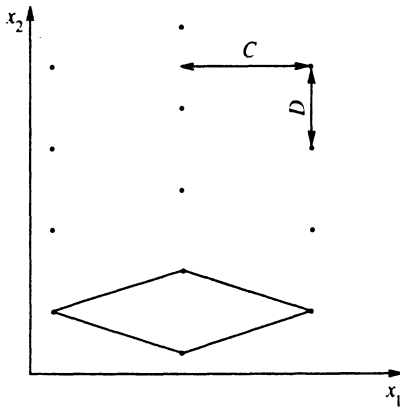


FIG. 3. Picture of the vortex lattice on the outer surface of the slab. The points represent the endpoints of the vortices. The unit cell (rhombus) is defined by the lattice parameters C and D .

3. These features of the vortex-vortex interaction afford a description of the magnetization of a thick HTSC slab. The vortex structure is completely determined by the two-dimensional lattice at the surface of the crystal and the shape of a bent vortex $\kappa_2(l_3)$. The curvature of the vortex lines cannot be measured directly in experiments; however, it is decisive in the formation of the lattice.

From the symmetry of the interaction [see expressions (8) and (18)] it follows that the equilibrium vortex lattice has rhombic symmetry. One of the mirror-symmetry axes should coincide with the direction of the field H_2 . Since the area of the unit cell is fixed and is equal to ϕ_0/B , the lattice on the surface of the slab can be described by just one parameter. Following Ref. 13, we define D to be the vortex spacing along the chains aligned with H_2 (see Fig. 3).

Separated vortices ($R \gg \mu_a^{-3/2}$) interact mainly through the vacuum. The long-range repulsion, which does not depend on the shape of the vortex lines, marshalls them into a regular triangular lattice. The exponentially weak anisotropic interaction tends to orient the lattice symmetrically about H_2 . But the influence of thermal fluctuations can be stronger, and for $B \ll \mu_a^{3/2} \phi_0$ a hexagonal lattice oriented arbitrarily in the plane of the film is observed.

The influence of anisotropy on the shape of the lattice begins to manifest itself as the vortex spacing decreases down to $R < \mu_a^{-3/2}$, when the vortex currents $j_3(\mathbf{x})$ begin to interact. In a sparse lattice, $B < \mu_a^3 \phi_0$, this takes place in strong planar fields, in which the equilibrium tilt of the vortices reaches the value $\kappa_2 \sim (\mu_a^3 \phi_0 / B)^{1/2}$. The mutual attraction of the vortices in a chain and the repulsion between chains causes the distance D to decrease. In contrast to the case of unbounded HTSC's, the decrease of D in the slab is small, thanks to the strong repulsion of the vortices at the surface. As the field H_2 grows the tilt of the vortices increases and reaches the value $\kappa_2 \sim \sqrt{\phi_0/B}$. For such a tilt the vortices in the chains are squeezed close together and neighboring vortices begin to repel each other. This leads to an increase of the parameter D .

Note that in an isotropic slab the vortices always repel

each other and as H_2 increases the distance D grows monotonically.

At large values of the magnetic induction $B > \phi_0$ the vortices are arrayed into a dense lattice and are aligned with the external field H . The anisotropic interaction between the central vortices contributes decisively to the formation of the lattice. As in the case of an unbounded superconductor,⁵ the shape of a dense vortex lattice can be described by the analytic expression

$$D = \sqrt{\frac{2\phi_0}{3B}} (1 + \mu_a^3 \tan^2 \theta)^{1/4}, \quad (23)$$

where θ is the tilt angle of the magnetic field. From this expression it is clear that for a constant magnetic induction B and increasing H_2 the lattice in an anisotropic superconductor remains hexagonal all the way to fields $H_2 \sim \mu_a^{-3/2} B$. With further increase of the field H_2 the distance D begins to grow.

In isotropic slabs the parameter D in dense lattices varies as $D \sim (\cos \theta)^{-1/2}$ if B is fixed, and $D \sim (\cos \theta)^{-1}$ if field H is constant in magnitude and tilted.

6. VORTEX STRUCTURES IN LAMINAR SAMPLES OF YBCO(123) AND BSCCO(2212)

1. Numerical calculation of the dependence $\kappa_2(x_3)$ for an isolated vortex in slabs of different anisotropy shows that the bending of the vortex takes place within a surface layer of thickness of the order of $\mu_a^{-3/4}$. In order to avoid having to solve the variational problem to determine $\kappa_2(x_3)$, we substitute a model shape for the actual shape of the vortex. We assume that the vortex consists of three rectilinear segments. The end segments have length $\mu_a^{-3/4}$ and are perpendicular to the surface, while the central segment is tilted with respect to H_2 ; its tilt is constant, $\kappa_2(x_3) = \kappa$.

The interaction of two vortices

$$U(\mathbf{R}) = U_1(\mathbf{R}) + U_2(\mathbf{R})$$

the long-range action of the end segments:

$$\begin{aligned} U_1(R) &= 2 \left(\frac{\phi_0}{4\pi} \right)^2 \int \frac{d^2 q}{2\pi} \left[\frac{1}{2(1+q^2)^{3/2}} + \frac{1}{q} - \frac{1}{(1+q^2)^{1/2}} \right. \\ &\quad \left. + \frac{\mu_a^{-3/4} - 1}{1+q^2} \right] \exp(i\mathbf{q}\mathbf{R}) \\ &= 2 \left(\frac{\phi_0}{4\pi} \right)^2 \left\{ \frac{2}{R} [1 - \exp(-R)] + \frac{1}{2} \exp(-R) \right. \\ &\quad \left. + (\mu_a^{-3/4} - 1) K_0(R) \right\}. \end{aligned}$$

The second term

$$\begin{aligned} U_2(\mathbf{R}) &= (d - 2\mu_a^{-3/4}) \left(\frac{\phi_0}{4\pi} \right)^2 \int \frac{d^2 q}{2\pi q^2} \left[\frac{q^2 + (\mathbf{q}\boldsymbol{\kappa})^2}{1 + q^2 + (\mathbf{q}\boldsymbol{\kappa})^2} \right. \\ &\quad \left. + \frac{[\mathbf{q}\boldsymbol{\kappa}]^2}{1 + q^2 \mu_a^{-3} + (\mathbf{q}\boldsymbol{\kappa})^2} \right] \exp(i\mathbf{q}\mathbf{R}) \end{aligned}$$

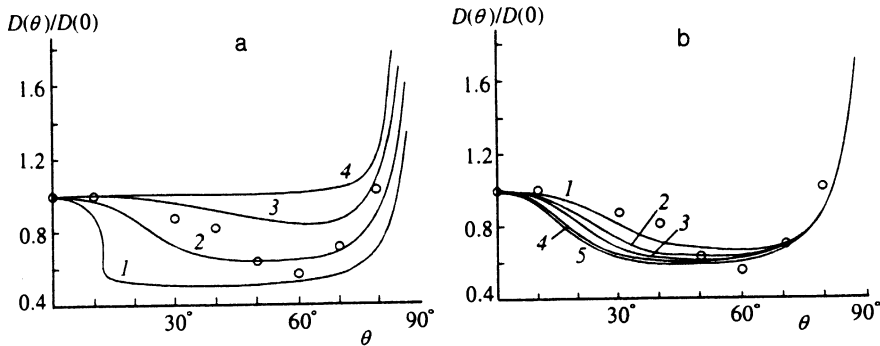


FIG. 4. Vortex spacing D along a chain versus the tilt angle θ of the external field \mathbf{H} for constant induction ($H \cos \theta = 12$ G). The points correspond to the experimental results,¹³ the curves—to theory: a) calculated for constant slab thickness $d=4 \mu\text{m}$ and various values of the anisotropy parameter: 1) 0.25, 2) 0.34, 3) 0.50, 4) 1.00; b) calculated for the anisotropy parameter held constant: $\mu_a=0.343$, while varying the thickness d : 1) $2 \mu\text{m}$, 2) $4 \mu\text{m}$, 3) $7 \mu\text{m}$, 4) $21 \mu\text{m}$, 5) $90 \mu\text{m}$.

describes the interaction of the central segments of the two vortices and coincides with the analogous expression for an unbounded crystal.²³

To determine the equilibrium parameters D and κ , we solved the corresponding equilibrium equations numerically.

2. We calculated the distance D in slabs of YBCO(123) for different values of the planar field. In order to compare the results with experiment¹³ we chose the following parameter values: $B=12$ G, $\lambda_a=0.14 \mu\text{m}$; the thickness of the slab d was varied from $2 \mu\text{m}$ to several tens of microns, and the anisotropy parameter μ_a took the following values: 1, 0.5, 0.343, and 0.25. The calculated function $D(\theta)$ is shown in Fig. 4 together with the experimental values. It can be seen that the best agreement is obtained at $\mu_a=0.343$ and small d .

These results confirm the qualitative treatment outlined in the previous section.

3. It is well known¹⁰ that in unbounded superconductors with $\mu_a < 1$ the intervortex attraction lowers the energy density of the vortex chain such that for $\mu_a < 0.28$ two types of chains can coexist. For fixed external field direction they differ in the vortex tilt κ and the vortex spacing D along the chains. The coexistence of different types of chains is possible only if the external field \mathbf{H} is tilted from the anisotropy axis by an angle smaller than 0.1° .

With the aim of discovering analogous metastable structures in HTSC slabs, we investigated BSCCO(2212), which has anisotropy $\mu_a=0.07$ (Ref. 3).

The results of this study, shown in Fig. 5, graphically demonstrate the existence of hysteresis in the magnetization of a slab of BSCCO(2212). In the angle interval $|\theta| < 20^\circ$ three equilibrium structures, differing among them-

selves in the parameters D and κ_2 . The stability of the given solutions depends on the sign of the two elastic moduli which describe the deformation of the vortex tilt toward the field \mathbf{H}_2 (the modulus T_{22}) and in the perpendicular direction (the modulus T_{11}). An expression for the moduli T_{11} in terms of the equilibrium dependence $\kappa_2(H_2)$ is obtained as follows:

$$G = n_L \left[F_0 + \sum_{\mathbf{R}}' U(\mathbf{R}) - \frac{1}{4\pi} \phi_0 H_2 \kappa_2 \right]. \quad (24)$$

The equilibrium equations have the form

$$\frac{\partial G}{\partial D} = 0, \quad \frac{\partial G}{\partial \kappa_2} = 0, \quad \frac{\partial G}{\partial \kappa_1} = \kappa_1 \left(\frac{1 + \kappa_2^2}{\kappa_2} \right) \frac{\partial G}{\partial \kappa_2} = 0.$$

The solution of these equations is $\kappa_1=0$, $\kappa_2=\kappa_2(H_2)$, $D=D(H_2)$. The small tilts of the field dH_2 cause small variations, $d\kappa$ and dD , in the equilibrium values of the parameters, which are determined by the equations

$$dD \sum' \frac{\partial^2 U}{\partial D^2} + d\kappa_2 \sum' \frac{\partial^2 U}{\partial D \partial \kappa_2} = 0,$$

$$d\kappa_2 \left[\frac{\partial^2 F_0}{\partial \kappa_2^2} + \sum' \frac{\partial^2 U}{\partial \kappa_2^2} \right] + dD \sum' \frac{\partial^2 U}{\partial D \partial \kappa_2} - dH_2 \frac{\phi_0}{4\pi} = 0.$$

The elastic tilt moduli, being second variational derivatives of the Gibbs potential (24), have the form

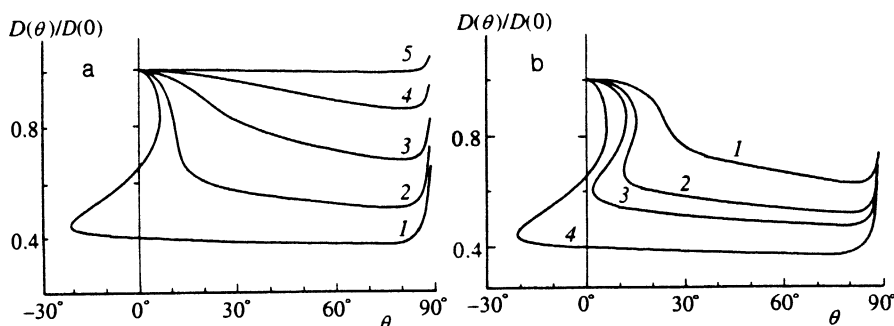


FIG. 5. Dependence of the vortex spacing $D(\theta)$ ($\lambda_a=0.07$): a) calculated results for a slab of thickness $d=40\lambda_a$ and various values of the induction $n_L \lambda_a^2$: 1) 0.01, 2) 0.02, 3) 0.04, 4) 0.10, 5) 1.00; b) calculated results in slabs of varying thickness d for the induction held fixed ($n_L \lambda_a^2=0.01$): 1) $16\lambda_a$, 2) $18\lambda_a$, 3) $20\lambda_a$, 4) $40\lambda_a$.

$$T_{11} = \frac{\partial^2 G}{\partial \kappa_1^2} = n_L \left(\frac{1 + \kappa_2^2}{\kappa_2} \right) \left[\frac{\partial F_0}{\partial \kappa_2} + \sum' \frac{\partial U}{\partial \kappa_2} \right] \\ = \frac{1 + \kappa_2^2}{\kappa_2} \frac{B H_2}{4\pi}, \quad (25)$$

$$T_{22} = \frac{\partial^2 G}{\partial \kappa_2^2} = n_L \left[\frac{\partial^2 F_0}{\partial \kappa_2^2} + \sum' \frac{\partial^2 U}{\partial \kappa_2^2} \right] \\ = \frac{B}{4\pi} \frac{dH_2}{d\kappa_2} - C_{\text{compr}} \left(\frac{dD}{d\kappa_2} \right)^2. \quad (26)$$

Here C_{compr} is the elastic compression modulus of the lattice at constant magnetic induction. Note that C_{compr} differs from the unilateral compression modulus, which in our problem becomes infinite. From Eq. (25) it can be seen that the stable vortex structures in Fig. 5 are located to the right of the ordinate $\theta=0$, i.e., the vortices are tilted toward the field H_2 . It follows from Eq. (26) that only the solutions with positive slope in the dependence $\kappa_2(H_2)$ are stable. The last term in (26) is always small and changes the value of T_{22} and the stability region of the metastable structures only insignificantly. Calculation of $\kappa_2(H_2)$ shows that in the hysteresis region the two extreme branches of $D(H_2)$ (the upper and the lower branch) are stable. The central branch is always unstable.

3. The results possess the following properties.

One of the metastable vortex structures is a weakly deformed hexagonal lattice with $D(\theta) \sim D(0)$, the other is a structure consisting of vortex chains. The vortex spacing along the chain $D(\theta)$ is much smaller than the interchain distance $C \sim D^2(0)/D(\theta)$.

The metastable structures exist at small values of the magnetic induction $B < 0.02 \phi_0 \lambda_a^{-2} \sim 3H_{c1}$. For BSCCO(2212) with $\lambda_a = 0.15 \mu\text{m}$ this corresponds to $B < 20$ G. As the induction increases (see Fig. 5a) the hysteresis region shifts toward larger angles θ , while its width decreases. There exists a critical value of the induction, which depends on the thickness of the slab, at which the hysteresis region disappears. The numerical solution for $B=1$ practically coincides with the analytic solution (23). Calculations carried out for $B=10$ and 30 confirm the conclusion (23) that for large values of the induction the shape of the vortex lattice $D(\theta)/D(0)$ does not depend on B .

The effect depends strongly on the thickness of the slab (see Fig. 5b). For a fixed value of the induction the hysteresis region decreases with decreasing slab thickness. There exists a critical thickness $d \sim 2\mu_a^{-1}$ below which metastable structures are not observed.

Note that in an unbounded single crystal of BSCCO(2212) hysteresis has been observed¹⁰ only for $\theta < 10^{-2}$ degrees.

Direct observation of vortex structures on the surface of slabs of BSCCO(2212) has shown¹⁴ that metastable vortex structures exist at significantly greater tilt angles of the external field, specifically, $\theta \sim 60^\circ$. It is possible that this difference between theory and experiment is due to oversimplification of the shape of the vortices.

7. CONCLUSION

In this paper we have investigated the influence of the finite dimensions of a HTSC crystal on the equilibrium shape of an isolated vortex and on different vortex structures. A vortex in a slab has a finite length, which varies with the degree of bending of the vortex. Bending of the vortex alters the vortex-vortex interaction potential substantially. Taking this circumstance into account affords a complete description of vortex structures in HTSC slabs, and in the case of YBCO(123) crystals it even allows one to achieve quantitative agreement between theory and experiment.¹³

In the present paper we have not considered the elastic properties of vortex lattices. However, the influence of the shape in this case is beyond doubt. In the first place, the elastic properties of a lattice with long-range action must be described with the help of the elasticity matrix.²⁴ The diagonal element that describes nonuniform compressional deformation should be proportional to the first power of the wave vector of the deformations. This means that on the surface of the crystal the lattice is practically incompressible while inside the crystal, by virtue of the short-range action of the vortices, arbitrary deformations of the lattice are possible. Second, for a sparse lattice the elastic moduli are not exponentially small. Consequently, the influence of thermal fluctuations on the stability of such a lattice is much less than predicted.²⁵ Tilt deformations are of special interest. By virtue of the finite length of the vortex and the fixed orientation of its ends (they are aligned with \mathbf{n}), the tilt deformation spectrum should be discrete. In addition to this discrete tilt spectrum there should exist a continuous shift spectrum. It is of great interest to us to examine the interaction of these two spectra due to the nondiagonal elastic moduli, predicted in Ref. 15.

The present work was partially supported by the Soros Fund of the American Physical Society (American Physical Society Grants and Scholarships Program for the Countries of the Former Soviet Union).

¹V. G. Kogan, Phys. Rev. B **38**, 7049 (1988).

²D. E. Farrell, C. M. Williams, S. A. Wolf, N. P. Bansal, and V. G. Kogan, Phys. Rev. Lett. **61**, 2805 (1988).

³D. E. Farrell, S. Bonham, J. Foster, Y. C. Chang, P. Z. Jiang, K. G. Vandervoort, D. G. Lam, and V. G. Kogan, Phys. Rev. Lett. **63**, 782 (1989).

⁴A. V. Balatskii, L. I. Burlachkov, and L. P. Gor'kov, Zh. Eksp. Teor. Fiz. **90**, 1478 (1986) [Sov. Phys. JETP **63**, 866 (1986)].

⁵V. G. Kogan, Phys. Rev. B **24**, 1572 (1981).

⁶L. J. Campbell, M. M. Doria, and V. G. Kogan, Phys. Rev. B **38**, 2439 (1988).

⁷A. M. Grishin, A. Yu. Martynovich, and S. V. Yampol'skiĭ, Preprint of Donetsk Phys.-Tech. Inst. No. 8, Donetsk (1988).

⁸G. J. Dolan, F. Holtzberg, C. Field, and T. R. Dinger, Phys. Rev. Lett. **62**, 2184 (1989).

⁹L. Ya. Vinnikov, I. V. Grigor'eva, L. A. Gurevich, and Yu. A. Osip'yan, Pis'ma Zh. Eksp. Teor. Fiz. **49**, 83 (1989) [JETP Lett. **49**, 99 (1989)].

¹⁰A. M. Grishin, A. Yu. Martynovich, and S. V. Yampol'skiĭ, Zh. Eksp.

- Teor. Fiz. **97**, 1930 (1990) [Sov. Phys. JETP **70**, 1089 (1990)].
- ¹¹O. Buisson and M. M. Doria, *Physica C* **181**, 273 (1991).
- ¹²A. I. Buzdin and A. Yu. Simonov, *Zh. Eksp. Teor. Fiz.* **98**, 2074 (1990) [Sov. Phys. JETP **71**, 1165 (1990)].
- ¹³P. L. Gammel, D. J. Bishop, J. P. Rice, D. M. Ginsberg, *Phys. Rev. Lett.* **68**, 3343 (1992).
- ¹⁴C. A. Bolle, P. L. Gammel, D. G. Grier, C. A. Murray, D. J. Bishop, D. B. Mitzi, and A. Kapitulnik, *Phys. Rev. Lett.* **62**, 112 (1991).
- ¹⁵A. M. Grishin, A. Yu. Martynovich, and S. M. Yampol'skii, *Zh. Eksp. Teor. Fiz.* **101**, 649 (1992) [Sov. Phys. JETP **74**, 345 (1992)].
- ¹⁶J. Pearl, *Appl. Phys. Lett.* **5**, 65 (1964).
- ¹⁷E. H. Brandt, *J. Mod. Phys. B* **5**, 751 (1991).
- ¹⁸V. V. Schmidt and G. S. Mkrtchyan, *Usp. Fiz. Nauk* **112**, 459 (1974) [Sov. Phys. Usp. **17**, 170 (1975)].
- ¹⁹A. L. Fetter and P. C. Hohenberg, *Phys. Rev.* **159**, 330 (1967).
- ²⁰O. Buisson, G. Garneiro, and M. M. Doria, *Physica C* **185-189**, 1465 (1991).
- ²¹I. M. Khalatnikov, *Theory of Superfluidity*, Nauka, Moscow (1971).
- ²²J. P. Hirth and J. Lothe, *Theory of Dislocations*, 2nd ed., Wiley, New York (1982).
- ²³V. G. Kogan, N. Nakagawa, and S. L. Tiemann, *Phys. Rev. B* **42**, 2631 (1990).
- ²⁴E. H. Brandt, *J. Low Temp. Phys.* **26**, 709 (1977).
- ²⁵D. S. Fisher, M. P. A. Fisher, and D. A. Huse, *Phys. Rev. B* **43**, 130 (1991).

Translated by Paul F. Schippnick